

# Lawrence Berkeley National Laboratory

## Recent Work

### Title

INCOMPLETE AND COMPLETE FUSION IN INTERMEDIATE ENERGY HEAVY ION REACTIONS

### Permalink

<https://escholarship.org/uc/item/8zr5383g>

### Author

Aleklett, K. .

### Publication Date

1984-05-01

2



# Lawrence Berkeley Laboratory

UNIVERSITY OF CALIFORNIA

LAWRENCE  
BERKELEY LABORATORY

JUL 24 1984

LIBRARY AND  
DOCUMENTS SECTION

Presented at the Fifth Nordic Meeting on Nuclear  
Physics, Jyvaskyla, Finland, March 12-16, 1984

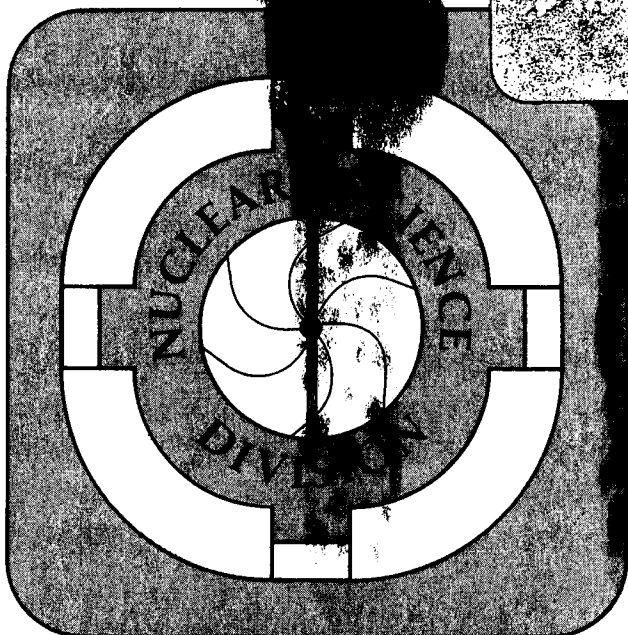
INCOMPLETE AND COMPLETE FUSION IN INTERMEDIATE  
ENERGY HEAVY ION REACTIONS

K. Aleklett, W. Loveland, T.T. Sugihara,  
D.J. Morrissey, L. Wenxin, W. Kot, and G.T. Seaborg

March 1984

**TWO-WEEK LOAN COPY**

*This is a Library Circulating Copy  
which may be borrowed for two weeks.*



LB1-17887

2

## **DISCLAIMER**

This document was prepared as an account of work sponsored by the United States Government. While this document is believed to contain correct information, neither the United States Government nor any agency thereof, nor the Regents of the University of California, nor any of their employees, makes any warranty, express or implied, or assumes any legal responsibility for the accuracy, completeness, or usefulness of any information, apparatus, product, or process disclosed, or represents that its use would not infringe privately owned rights. Reference herein to any specific commercial product, process, or service by its trade name, trademark, manufacturer, or otherwise, does not necessarily constitute or imply its endorsement, recommendation, or favoring by the United States Government or any agency thereof, or the Regents of the University of California. The views and opinions of authors expressed herein do not necessarily state or reflect those of the United States Government or any agency thereof or the Regents of the University of California.

Incomplete and Complete Fusion in Intermediate Energy  
Heavy Ion Reactions

K. Aleklett  
Studsvik Science Research Laboratory  
S-611 82 NYKÖPING, Sweden

W. Loveland and T.T. Sugihara  
Oregon State University, Corvallis, OR 97331, USA

D.J. Morrissey  
Michigan State University, MI 48824, USA

Li Wenxin, Wing Kot and G.T. Seaborg  
Lawrence Berkeley Laboratory, University of California  
Berkeley, CA 94720, USA

This work was supported by the Director, Office of Energy Research, Division of Nuclear Physics of the Office of High Energy and Nuclear Physics of the U.S. Department of Energy under Contract DE-AC03-76SF00098.

Incomplete and Complete Fusion in Intermediate Energy  
Heavy Ion Reactions

K. Aleklett  
Studsvik Science Research Laboratory  
S-611 82 NYKÖPING, Sweden

W. Loveland and T.T. Sugihara  
Oregon State University, Corvallis, OR 97331, USA

D.J. Morrissey  
Michigan State University, MI 48824, USA

Li Wenxin, Wing Kot and G.T. Seaborg,  
Lawrence Berkeley Laboratory, Berkeley, CA 94720, USA

Abstract

The yields, angular distributions and differential range spectra have been measured for individual target residues from the interaction of 8.5 MeV/A  $^{16}\text{O}$ , 19 MeV/A  $^{16}\text{O}$ , 35 MeV/A  $^{12}\text{C}$  and 86 MeV/A  $^{12}\text{C}$  with  $^{154}\text{Sm}$ . From the measured data, fragment isobaric yields and velocity spectra were deduced. The results are compared to the sum rule model of Wilczyski et al. and the nuclear firestreak model.

1. Introduction

In recent years, considerable interest has developed in characterizing nucleus-nucleus collisions in the intermediate energy regime (20-100 MeV/A). A number of studies have measured the average linear momentum transfer to the target nucleus in these collisions. The situation has been characterized in a systematics of average fractional momentum transfer, similar to the one developed by Viola et al.<sup>1)</sup> and Stockstad et al.<sup>2)</sup>, which is shown in Figure 1. Also shown in Figure 1 are other data<sup>3-6)</sup> which extend this correlation to higher energies. As the data of Figure 1 show, the average fraction of the beam momentum transferred to the target nucleus decreases approximately linearly with increasing relative velocity of the colliding

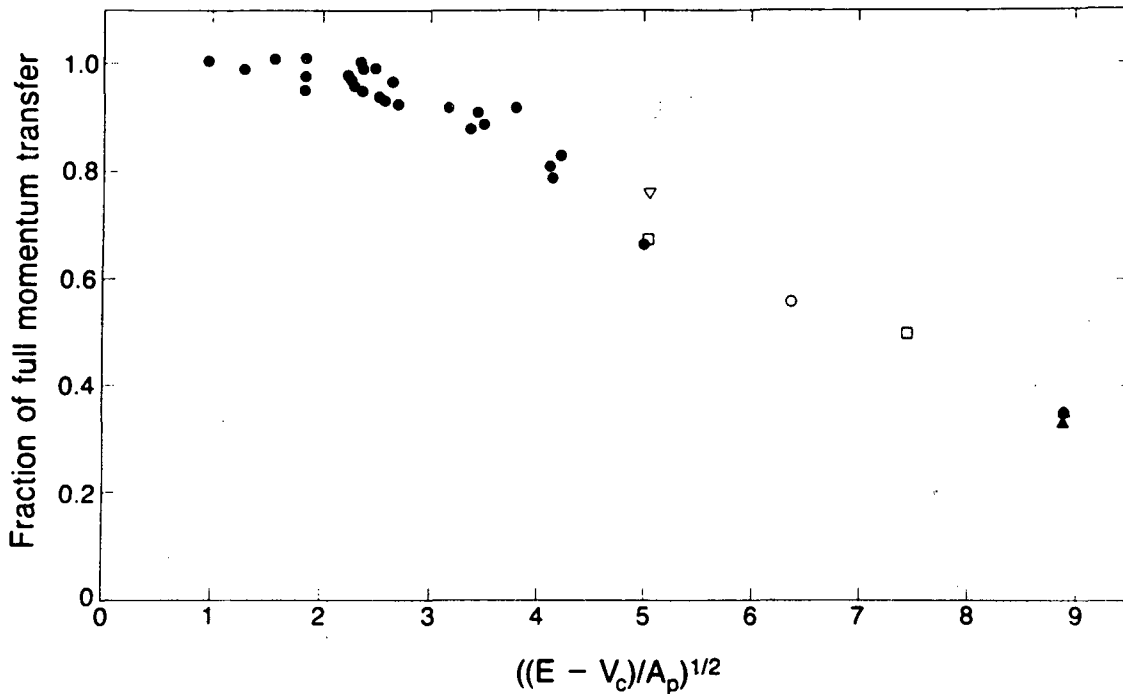


Figure 1. Fraction of beam momentum transferred to target nucleus in nucleus-nucleus collisions leading to fission or residue production as a function of the relative velocity of the colliding ions. Filled circles are data from Ref. 1 and 2, open circles--Ref. 3, filled triangles--Ref. 4, squares--Ref. 5, open triangles--Ref. 6.

nuclei. As the projectile energy increases, incomplete fusion processes become increasingly important and it is worth noting that throughout this energy regime, the average fractional linear momentum transfer significantly exceeds that observed in relativistic nuclear collisions<sup>3)</sup>.

As informative as these measurements are, we felt that it would be useful to study the evolution of individual reaction channels rather than "average" behavior as a function of projectile energy for intermediate energy nucleus-nucleus collisions. In addition, we were intrigued by reports<sup>7)</sup> of production of trans-target species with large probability (for  $\Delta Z = + 1$ ,  $\sigma = 200 - 250$  mb) in the reaction of 86 MeV/A  $^{12}\text{C}$  with lead and bismuth. According-

ly, we decided to begin a systematic study of the yields, angular distributions and velocity spectra (using differential range techniques) of target residues from the interaction of intermediate energy heavy ions with the n-rich rare earth targets  $^{150}\text{Nd}$ ,  $^{154}\text{Sm}$ , and  $^{176}\text{Yb}$ . Through the use of the n-rich rare earth targets we should severely repress the "masking effects" of the fission of any target residues or transfer products. In this paper we present a preliminary report of the data obtained for the interaction of intermediate energy heavy ions with  $^{154}\text{Sm}$ .

## 2. Experimental

We have measured the yields, angular distribution and differential range spectra for target residues formed in the interaction of 8.5 MeV/A  $^{16}\text{O}$ , 19 MeV/A  $^{16}\text{O}$ , 35 MeV/A  $^{12}\text{C}$  and 86 MeV/A  $^{12}\text{C}$  with  $^{154}\text{Sm}$ . The irradiations with the 8.5 and 19 MeV/A  $^{16}\text{O}$  were carried out at the LBL 88" cyclotron, while the irradiations with 35 MeV/A and 86 MeV/A  $^{12}\text{C}$  were performed at the MSU superconducting cyclotron and the CERN SC synchrocyclotron, respectively. Targets consisting of deposits of  $^{154}\text{Sm}_2\text{O}_3$  (98.7 %  $^{154}\text{Sm}$ ) of various thicknesses ranging from 0.3 to 1.0 mg/cm<sup>2</sup> on a 4.7 mg/cm<sup>2</sup> Be backing were irradiated for times of 3 - 7 hours with heavy ion beams ranging in intensity from  $10^{10}$ - $10^{12}$  ions/sec. In the differential range measurements, all fragments recoiling from the target in the forward hemisphere were stopped in a stack of Al foils of various thicknesses (0.25-1.6 mg/cm<sup>2</sup>). In the angular distribution measurements, fragments emerging from the target were stopped in a cylindrical arrangement of catcher foils. Fragments emerging at 0-10° with respect to the incident beam were caught in a 35 mg/cm<sup>2</sup> C foil while fragments with  $10^\circ \leq \theta \leq 60^\circ$  were caught in 17.6 mg/cm<sup>2</sup> mylar catchers.

Following irradiation, the catcher foils from the angular distribution measurements were cut into pieces representing various angular intervals. These pieces along with the individual foils from the differential range

measurements and the target foils were assayed by  $\gamma$ -ray spectroscopy beginning a few minutes after end of irradiation and continuing for periods of up to 3 months in laboratories at MSU and LBL. The identification of the activities present in each foil and the calculation of cross sections from these measured activities has been described previously<sup>8)</sup>. The total activity found in the target and catcher foils was used in calculating the nuclidic production cross sections.

In the angular distribution experiments, the resolution of the experiments was detected primarily by the angular width of the catcher foils (the beam spot size was  $< 4 \text{ mm}^2$ ). The alignment and centering of the beam was checked prior to the irradiation, during the irradiation and after the irradiation using radiography and on-line monitoring devices. No correction was made to the measured data for the finite angular resolution of the catcher foils because it was not felt to be critical for understanding the physics revealed by the data. The effect of the finite target thickness upon the measured angular distributions has been evaluated recently for a similar study<sup>9)</sup>. Stopping of the fragments in the target or large angle scattering in the target can be excluded although there is probably some smearing of the angular distributions due to small angle scattering in the target.

Because of very strongly forward-peaked character of the angular distributions, the projected range distributions measured in the differential range experiments are, in fact, the true range distributions. Using the range-velocity relationships of Northcliffe and Schilling<sup>10)</sup>, the differential range distributions were converted to invariant velocity distributions. (These range-velocity relationships have been previously shown<sup>11)</sup> to be accurate to a few per cent for ions of the same Z, A and energy as encountered in this study). No attempts have been made at this stage of the data analysis to correct for the effects of range straggling upon the data.



### 3. Phenomenological Models

To help understand the significant features of the data, we have chosen to compare our data with two phenomenological models of intermediate energy nucleus-nucleus collisions. The first of these models is the generalized sum rule model of Wilczynski et al.<sup>12)</sup>. The adjustable parameters in the model calculation ( $T$ ,  $\Delta\ell$ , etc.) were the same as used by Wilczynski et al.<sup>12)</sup>. The excitation energy of each of the possible target residues was assumed to be the "optimal" excitation energy as calculated using a semi-classical DWBA of Toeppler<sup>13)</sup> (previously used by Hubert et al.<sup>14)</sup> to calculate the yields of transfer products in low energy reactions). The deexcitation of each primary fragment was calculated using a version<sup>15)</sup> of the DFF code.

The data are also compared with the predictions of the nuclear firestreak model<sup>15, 16)</sup>. In this model, the colliding nuclei are assumed to have diffuse surfaces, which were generated by folding a short-range (Yukawa) function into the conventional sharp-sphere density distribution. It was assumed that during the collision the interaction was localized to the overlap region, where collinear tubes of nuclear matter from the target and projectile underwent completely inelastic collisions. A transparency function, based upon a fixed nucleon-nucleon scattering cross-section of 30 mb, was included to prevent collisions from occurring between tubes containing an insufficient density of nucleons.

Once two tube have collided, they are assumed to fuse and equilibrate their kinetic and thermal energies. If the resulting kinetic energy of a fused tube is less than its binding energy in the target remnant, then it is retained and contributes directly to the remnant's energy, mass, and momenta, which are explicitly conserved during the interaction. The calculation of how the primary fragment distributions predicted by this model de-excited were done using the same DFF code as for the Wilczynski model.

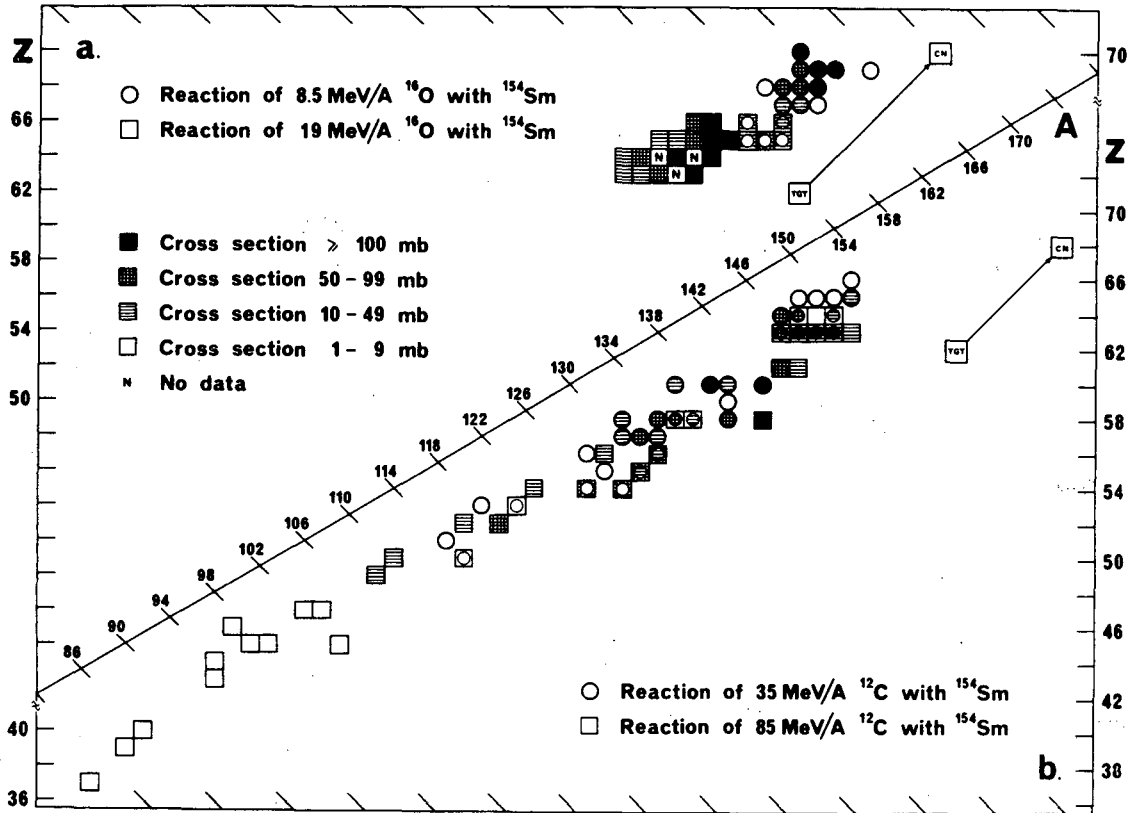


Figure 2. Plot of nuclidic yields for the reaction of a) 8.5 MeV/A and 19 MeV/A  $^{16}\text{O}$  with  $^{154}\text{Sm}$ , and b) 35 MeV/A and 86 MeV/A  $^{12}\text{C}$  with  $^{154}\text{Sm}$ .

#### 4. Results

The individual target fragment yields for the reaction of heavy ions with  $^{154}\text{Sm}$  are shown in Figure 2 while the isobaric yields derived from integrating the individual nuclidic yields while correcting for  $\beta$ -decay and unobserved species<sup>17)</sup> are shown in Figure 3. In both figures, one can see the qualitative changes in reaction mechanism as the projectile energy increases. At the lowest energy (8.5 MeV/A), the fragment yield distribution is sharply peaked at a mass number near that of the completely fused system, with most of the reactions proceeding via a complete fusion mechanism. As the projectile energy increases, so does the

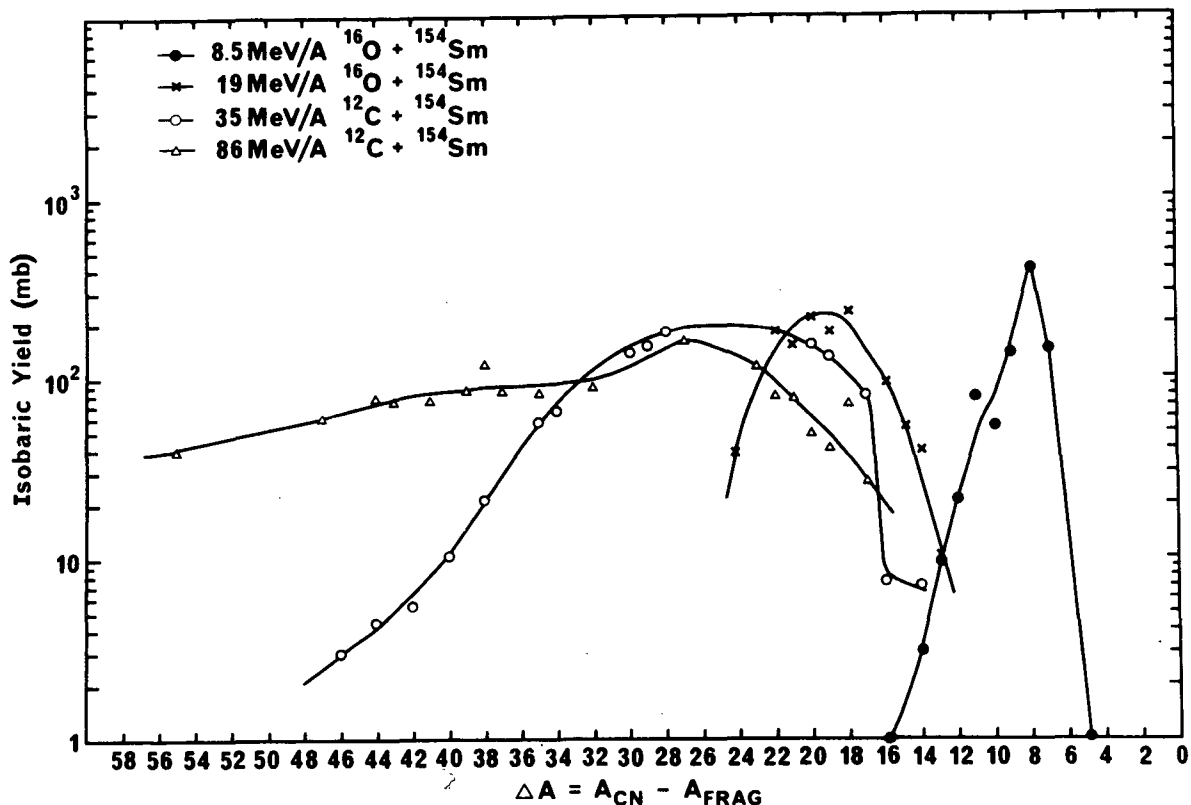


Figure 3 Fragment isobaric yield distributions for the reaction of various heavy ions with  $^{154}\text{Sm}$ . The lines are to guide the eye through the data points.

energy deposited in the target nucleus, leading to the production (after deexcitation) of fragments of lower and lower mass numbers. Correspondingly, the fragment isobaric yield distribution becomes broader - but the decrease in the mass transfer from projectile to target nucleus causes the isobaric yield distribution to be asymmetric with a steeper upper edge and a long "spallation-like" tail towards lower masses. It is interesting to note that even at a projectile energy of 86 MeV/A, significant formation of trans-target species is observed although with somewhat less probability than in the reaction of 86 MeV/A  $^{12}\text{C}$  with  $^{206}\text{Pb}$ ,  $^{209}\text{Bi}$  7).

It is interesting to compare these data with the predictions of the two phenomenological models discussed previously (Figure 4). The sum rule model generally describes the shape of the isobaric distribution at a projectile energy of 8.5 MeV/A (apart from a small peak at A

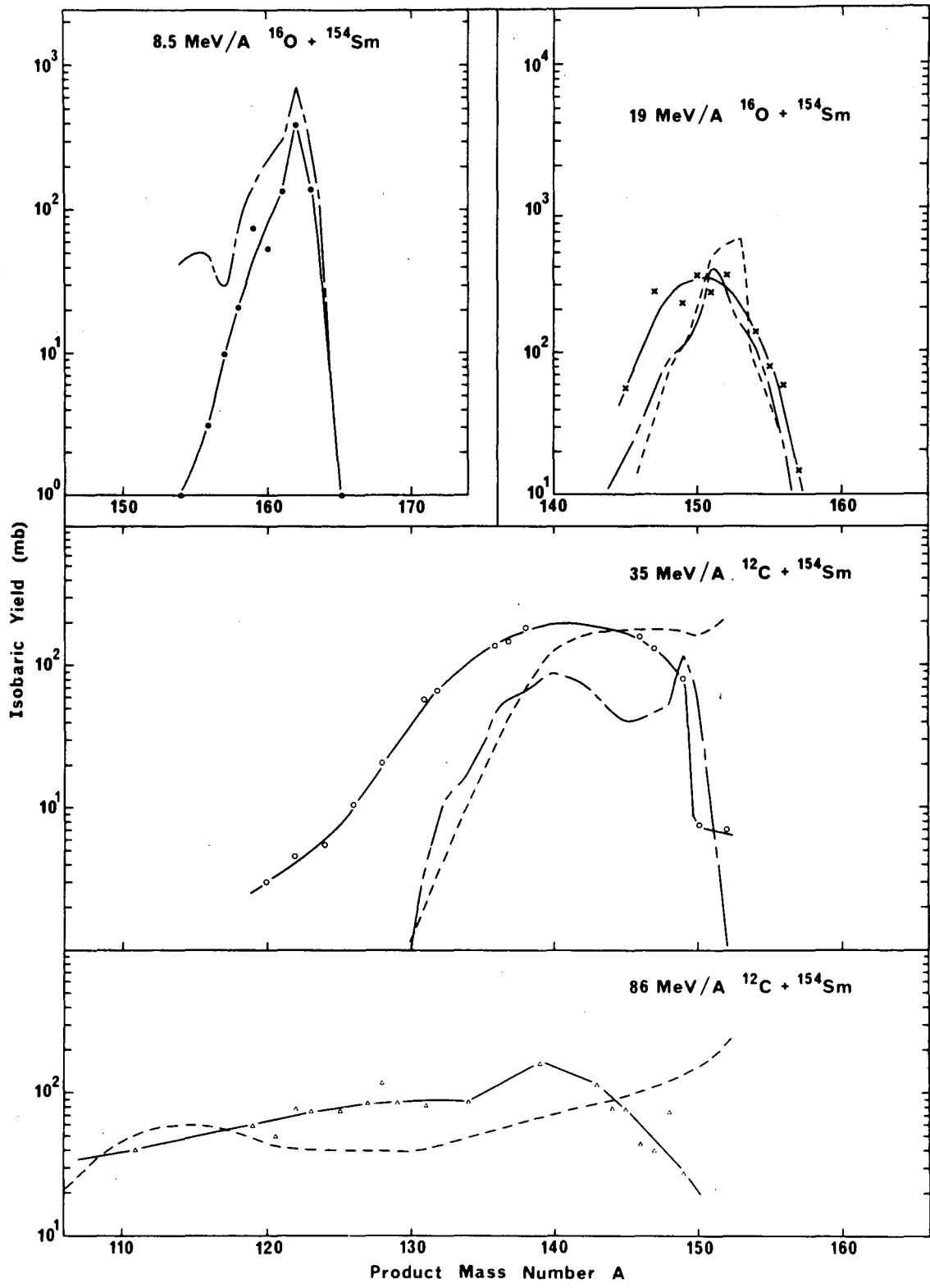


Figure 4. Comparison of measured isobaric yield distributions with those predicted by the sum rule model (dashed curve) and firestreak model (long line-dash curve).

~155 which in the model is due to  $\alpha$ -transfer reactions) but overestimates the magnitude of the cross sections. As the projectile energy increases, this model fails to account for the observed broadening of the isobaric distribution.

The nuclear firestreak model has been used successfully to account for fragment yields in reactions induced by relativistic heavy ions. However, there is significant disagreement between the predictions of this model and the isobaric yield data. At the highest projectile energy, the yields of fragments of high A are overestimated. The peak in the predicted distribution at  $A \sim 114$  (which is not observed) is due to the deexcited quasi-compound nucleus. Thus it should seem that the model overestimates the occurrence of both very low and very high mass transfer events. As the projectile energy is lowered, the predicted distributions mimic some general features of the data but only in a crude, qualitative manner. These failures of the firestreak model were not seen in comparisons of predicted and measured isobaric yield distributions in the reaction of intermediate energy heavy ions with  $\text{Au}^{3)}$  and  $\text{U}^{15)}$ . But in those cases, a significant fraction of the events resulted in fission and thus a less stringent test of the model was possible.

Another view of the changes in reaction mechanism with projectile energy can be obtained by examining a representative set of invariant velocity spectra. At the lowest projectile energy, (8.5 MeV/A  $^{16}\text{O}$ ), the velocity spectra show Gaussian peaks centered near the velocity of the completely fused system (Figure 5a). If we take the number of those events with  $V > V_{\text{CN}}$  and double this number, assuming a Gaussian peak, we get a measure of the cross section for complete fusion (neglecting range straggling effects). For the interaction of 8.5 MeV/A  $^{16}\text{O}$  with  $^{154}\text{Sm}$ , 93 % of the cross section is estimated to be associated with complete fusion reactions. Also, as seen in figure 4, the measured average fragment velocity for a typical fragment,  $^{163}\text{Tm}$ , agrees well with that value predicted by the Wilczynski et al. sum rule model.

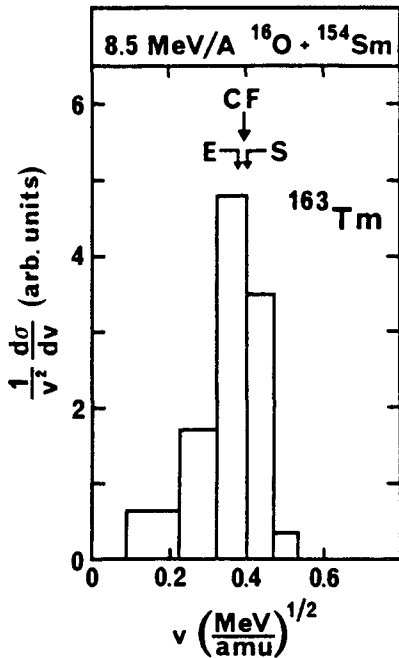


Figure 5a. Representative velocity spectra for fragments from the reaction of intermediate energy heavy ions with  $^{154}\text{Sm}$ . The arrows indicate the mean residue velocity such that CF corresponds to complete fusion, E the mean measured velocity, S the average velocity as predicted by the sum rule model, and F the average velocity predicted by the fire-streak model.

For the reaction of 19 MeV/A  $^{16}\text{O}$  with  $^{154}\text{Sm}$ , the velocity spectrum of  $^{151}\text{Tb}$  represents that of a typical product (Figure 5 b). The mean fragment velocity agrees well with the sum rule and firestreak model predictions and is considerably less than that of a completely fused system. The velocity spectrum of  $^{151}\text{Tb}$  can be thought of as a composite of spectra representing different reaction mechanisms, such as the spectra shown for  $^{151}\text{Gd}$  (very incomplete fusion) and  $^{156}\text{Tb}$  (near complete fusion). Using the same methods as before, we can estimate that  $\sim 35\%$  of the reactions proceed by a complete fusion mechanism.

For the reaction of 35 MeV/A  $^{12}\text{C}$  with  $^{154}\text{Sm}$ , three typical fragment velocity spectra are shown (Figure 5b). The nuclides involved represent different portions of the yield distribution for this reaction. All spectra show considerable amounts of incomplete fusion with mean fragment velocities being  $\sim 1/2$  that of the completely fused system. The fraction of events leading to complete fusion is  $< 5\%$ . The Wilczynski *et al.* sum rule and the firestreak model overestimate (usually by a large amount) the mean fragment velocities.

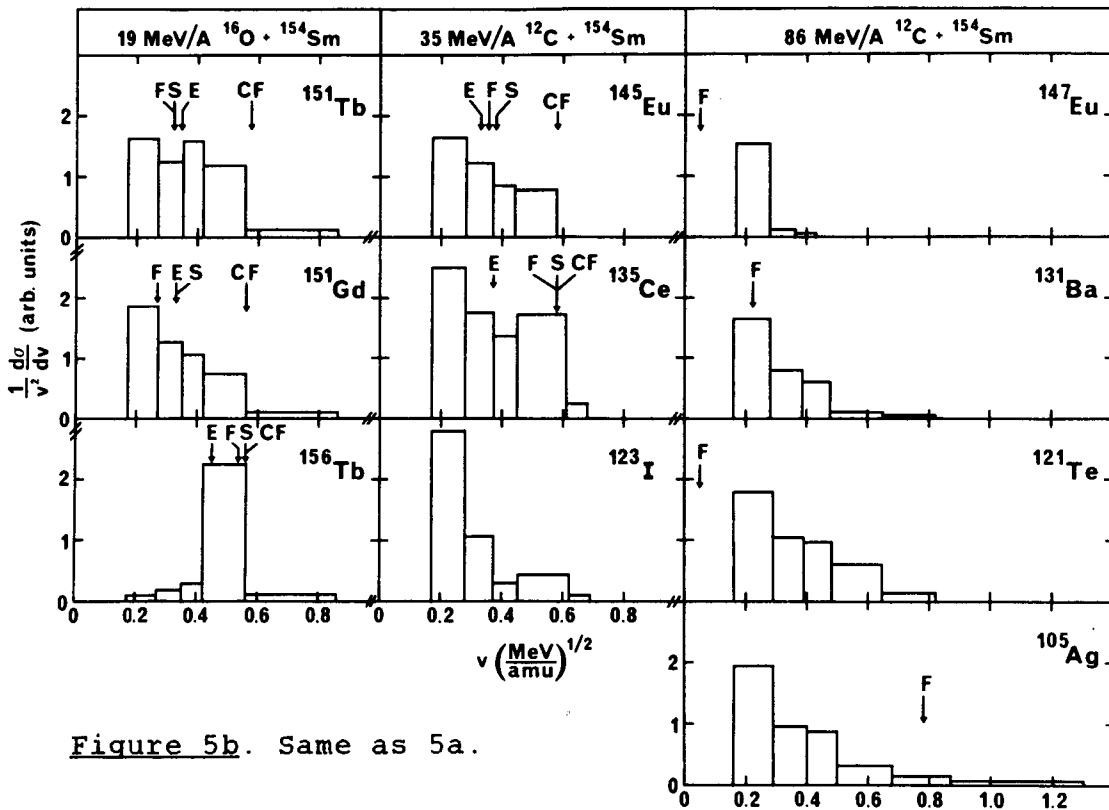


Figure 5b. Same as 5a.

The continually worsening accord between the predictions of the models and the data as the projectile energy increases is due in part to an overestimation of the magnitude of the complete fusion cross section by the models. Trajectories (or impact parameters) leading to complete fusion at 8.5 MeV/A projectile energy simply do not lead to complete fusion at 35 MeV/A, as the model generally assumes, nor is the projectile stopped in the target in some events as the firestreak model predicts.

At 86 MeV/A, the velocity spectra of all typical products are dominated by incomplete fusion. The trans-target species  $^{147}\text{Eu}$  shows the smallest velocities while the number of events with higher velocities (more "complete" fusion, harder collisions) increases with decreasing fragment mass. Thus the production of trans-target species in the reaction of 86 MeV/A  $^{12}\text{C}$  with heavy targets involves events with very small momentum (and energy) transfer allowing their survival even when produced in reactions involving moderately fissionable targets such as Pb and Bi.

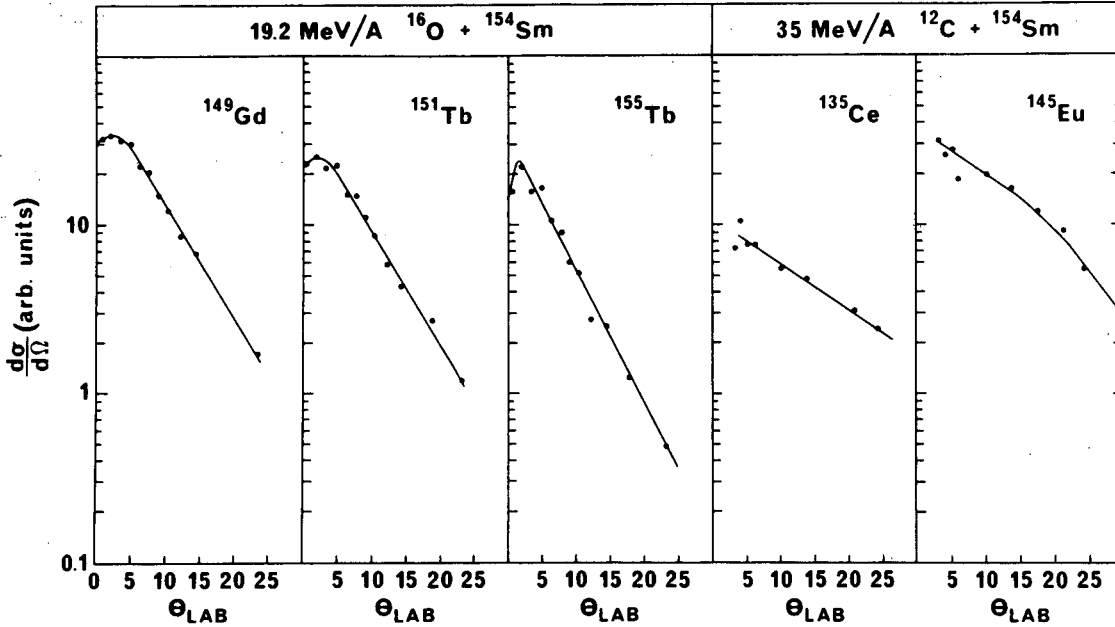


Figure 6. Typical laboratory system fragment angular distributions.

Representative fragment angular distributions for the reactions of 19 MeV/A and 35 MeV/A with  $^{154}\text{Sm}$  are shown in Figure 6. The angular distributions for the reactions involving 35 MeV/A  $^{12}\text{C}$  are generally broader than those measured at 19 MeV/A due in part to the increased particle emission because of the larger energy deposit in the higher energy reaction. This can be shown by remembering that the mean square dispersion in the heavy fragment recoil angle,  $\overline{\theta_L^2}$ , due to particle emission is given by<sup>18)</sup>

$$\overline{\theta_L^2} = \frac{2}{3} \left( \frac{V}{v} \right)^2 \quad (1)$$

if one assumes that particle emission is isotropic in the moving frame.  $V$  is the velocity of the recoil in the moving frame (due to kicks given it by particle emission) while  $v$  is the velocity of the moving frame (i.e., the velocity given the heavy product in the primary nuclear reaction to particle emission).

$v$  can be taken as the mean projected fragment velocity



as measured in the differential range experiments while  $V$  is given by<sup>18)</sup>

$$\frac{\pi}{4} \left( \frac{V}{v} \right) = \overline{\theta_L} \quad (2)$$

where  $\overline{\theta_L}$  is the mean recoil angle. Use of equations (1) and (2) allows one to predict values of  $\overline{\theta_L^2}$  of 0.022 rad<sup>2</sup>) for <sup>149</sup>Gd and 0.0866 rad<sup>2</sup>) for <sup>135</sup>Ce produced in the 19 MeV/A and 35 MeV/A reactions, respectively. These numbers are to be compared to the measured dispersions of 0.0267 rad<sup>2</sup> for <sup>149</sup>Gd and 0.118 rad<sup>2</sup>) for <sup>135</sup>Ce. Thus it would seem that a major portion of the dispersion in the angular distributions is due to particle emission.

#### 5. Summary and Conclusions

The preliminary data from this survey of incomplete fusion at intermediate energies shows the importance of incomplete fusion reactions in this energy regime. Production and survival of trans-target species occurs with significant probability at all projectile energies surveyed. The Wilczinski et al. sum rule model becomes less effective at describing the incomplete fusion reactions as the projectile energy increases and the nuclear firestreak model also seems to fail to properly describe the observed distributions in this energy regime.

#### Acknowledgements

This work was supported in part by the US Department of Energy under Contract DE-AC03-76SF00098 and DE-AM06-76RLO2227, Task Agreement DE-ATO6-76ER70035, Mod A007, the National Science Foundation and the Swedish Natural Science Research Council. We gratefully acknowledge the aid of the operations staff and health physics staff of the accelerators at LBL, MSU and CERN, Nuclear Data Inc. for loaning us equipment, Mr. P. Wilmarth of LBL and Mr. Jack Hernandez of Texas A & M for assistance in target prepara-

tion, and the members of the SHEIKS group for assistance in counting samples. Both KA and WDL wish to acknowledge the hospitality of the Lawrence Berkeley Laboratory during the time in which the experiments were performed and WDL wishes to further acknowledge the hospitality of the Studsvik Science Research Laboratory during preparation of this manuscript.

### References

1. Viola, V.E., Jr., Back, B.B., Wolf, K.L., Awes, T.C., Gelbke, C.K., and Breuer, H., Phys. Rev. C26 (1982) 178; Viola, V.E., Jr., Clark, R.G., Meyer, W.G., Zebelman, A.M., and Sextro, R.G., Nucl. Phys. A261 (1976) 174.
2. Stokstad, R.C., Chan, Y., Murphy, M., Tserruya, I., Wald, S., and Budzanowski, A., Lawrence Berkeley Laboratory Report LBL-15874, (1983).
3. Loveland, W., Aleklett, K., McGaughey, P.L., Moody, K.J., McFarland, R.M., Kraus, R.H., Jr., and Seaborg, G.T., Phys. Rev. V (submitted for publication).
4. Lynen, U., Ho, H., Kuhm, W., Pelte, D., Winkler, U., Møller, W.F.J., Chu, Y.T., Doll, P., Gobbi, A., Hildebrand, K., Olmi, A., Stelzer, H., Bock, R., Lohner, H., Glasow, R., and Santo, R., Nucl. Phys. A387 (1982) 129c.
5. Galin, J., Oeschler, H., Song, S., Borderie, B., Rivet, M.F., Forest, I., Bimbot, R., Gardes, D., Gatty, B., Guillemot, H., Lefort, M., Tamain, B., and Trrago, X., Phys. Rev. Lett. 48 (1982) 1787; Rivet, M.F., Borderie, B., Song, S., Guerreau, D., Oeschler, H., Bimbot, R., Forest, I., Galin, J., Gardes, D., Gatty, B., Lefort, M., Tamain, B., and Tarrago, X., Nucl. Phys. A387 (1982) 143C.
6. Nebbia, G., Tomasi, E., Ngo, C., Chen, X.S., LaRama, G., Leray, S., Lhenoret, P., Lucas, R., Mazur, C., Ribag, M., Cerruti, C., Chiodelli, S., Demeyer, A., Guinet, D., Charvet, J.L., Morjian, M., Pranal, Y., Peghaire, A., Sinopoli, L., Uzureau, J., and de Swiniarski, R., Z. Phys. A311 (1983) 247.
7. Molzahn, D., Lund, T., Brandt, R., Hagebø, E., Haldorsen, I.R., and Serre, C.R., J. Radioanal. Chem. 80, (1983) 109.
8. Morrisey, D.J., Lee, D., Otto, R.J., and Seaborg, G.T., Nucl. Instr. Meth. 158, (1978) 499.
9. Kraus, Jr., R.H., Loveland, W., Aleklett, K., McGaughey, P.L., Sugihara, T.T., Seaborg, G.T., Lund, T., Morita, Y., Hagebø, E., and Haldorsen, I.R., Nucl. Phys. A. (submitted for publication).

10. Northcliffe, L.C., and Shilling, R.F., Nucl. Data Tables, 1, (1970) 233.
11. Winsberg, L., and Alexander, T., Phys. Rev. 121, 518 (1961).
12. Wilczynski, J., Siwek-Wilczynska, K., van Drill, J., Gonggrizp, S., Hageman, D.C.J.M., Janssens, R.V.F., Lukasiak, J., and Siemonsen, R.H., Phys. Rev. Lett. 45, (1980) 606.
13. Toepffer, C., Z. Physik 253, (1972) 78.
14. Hubert, F., Delagrange, H., and Fleury, A., Nucl. Phys. A22B, (1974) 415.
15. McGaughey, P.L., Lawrence Berkeley Laboratory Report LBL-15325, November, 1982.
16. Myers, W.D., Nucl. Phys. A296, (1978) 177.
17. Morrissey, D.J., Loveland, W., de Saint-Simon, M., and Seaborg, G.T., Phys. Rev. C21 (1980) 1783.
18. Alexander, J.M. in Nuclear Chemistry, Vol. I., Yaffe, L. Ed. (Academic Press, New York, 1968) p. 273.

Acknowledgment:

This work was supported by the Director, Office of Energy Research, Division of Nuclear Physics of the Office of High Energy and Nuclear Physics of the U.S. Department of Energy under Contract DE-AC03-76SF00098.

This report was done with support from the Department of Energy. Any conclusions or opinions expressed in this report represent solely those of the author(s) and not necessarily those of The Regents of the University of California, the Lawrence Berkeley Laboratory or the Department of Energy.

Reference to a company or product name does not imply approval or recommendation of the product by the University of California or the U.S. Department of Energy to the exclusion of others that may be suitable.

TECHNICAL INFORMATION DEPARTMENT  
LAWRENCE BERKELEY LABORATORY  
UNIVERSITY OF CALIFORNIA  
BERKELEY, CALIFORNIA 94720